

Experimental Signatures of the Gauge-Higgs Unification Models

A.A. Babich *

Sukhoi State Technical University of Gomel

Abstract

The phenomenological predictions of the 5D gauge-Higgs unification models with $SO(5) \times U(1)$ gauge group, where the fifth dimension is compactified on an orbifold S^1/Z_2 , are discussed. Shown that the discovery of the two Z' bosons with close masses in experiments at LHC would give strong support for the gauge-Higgs unification and signal about the existence of extra dimensions.

1 Introduction

After the discovery of a Higgs boson at LHC [1]-[2] many fundamental questions remains unresolved still now. One of such questions is the hierarchy problem. Gauge-Higgs Unification (GHU) is one of the attractive scenarios beyond the Standard Model, which provide a possible solution to the hierarchy problem without supersymmetry. In this scenario, the SM Higgs boson and the gauge fields are unified into higher dimensional gauge fields. A remarkable fact is that the quantum corrections to Higgs mass and potential are UV-finite and calculable due to the higher dimensional gauge symmetry though the theory may be the non-renormalizable!

The fact that the Higgs boson is a part of gauge fields implies that Higgs interactions are governed by gauge principle and may provide specific predictions in LHC physics.

*E-mail: babich@gstu.gomel.by

2 Realistic GHU models

The idea of the gauge-Higgs unification is rather old and the one was proposed by Fairlie and by Forgacs and Manton in 1979 [3]-[6].

The first attempts have been based on embedding the SM electroweak gauge group $SU(2)_L \times U(1)_Y$ to the large simple group \mathcal{G} and thus gauge fields live in spacetime with $M^4 \times S^2$ topology. But unfortunately the models in a simple variant were unrealistic as predicted too small higgs boson mass and an incorrect the Weinberg angle θ_W (see Table 1).

\mathcal{G}	$\sin^2 \theta_W$	m_W	m_Z	m_H
$SU(3)$	3/4	44 GeV	88 GeV	88 GeV
$O(5)$	1/2	54 GeV	76 GeV	76 GeV
G_2	1/4	76 GeV	88 GeV	88 GeV

Table 1: Spectrum in the Gauge-Higgs Unification model by Manton.

New attempts of construction of realistic models are based on realization of several key ideas, such as orbifolds, warped spacetime, Hosotani mechanism of dynamical breaking gauge symmetry and some other.

Further we will shortly characterize the most promising realistic models [7]-[11].

All of these models are formulated as 5D GHU models with $SO(5) \times U(1)_X$ gauge group, where the fifth dimension is compactified on an orbifold S^1/Z_2 with a compactification radius R . The models do not contradict all precise electroweak experimental data and differ from each other by structure of fermion sector.

The gauge group choice as $SO(5) \times U(1)_X$ is caused by following reason. At first, in the EW symmetry breaking $SU(2)_L \times U(1)_Y \rightarrow U(1)_{EM}$ the Higgs field is an $SU(2)_L$ doublet in the fundamental representation. In the Gauge-Higgs Unification scheme the Higgs field is a part of gauge fields which are in the adjoint representation of the gauge group \mathcal{G} . So this implies that one needs to start with a larger gauge group \mathcal{G} which contains $SU(2)_L \times U(1)_Y$ as a subgroup. At second, group $SO(5)$ is minimal group which contain SM custodial symmetry group $SO(4) \cong SU(2)_L \times SU(2)_R$ as subgroup that allows to make control over the corrections to S and T electroweak parameters. And at third, factor $U(1)_X$ allows to make control over the correct value of Weinberg angle due to additional gauge coupling

constant.

The models are defined in the 5D Randall-Sundrum (RS) warped space $M^4 \times S^1/Z_2$ with orbifold topology in the fifth dimension. The metric is written as

$$ds^2 = e^{-2\sigma(y)} \eta_{\mu\nu} dx^\mu dx^\nu + dy^2, \quad (1)$$

where $\eta_{\mu\nu} = \text{diag}(-1, 1, 1, 1)$, $\sigma(y) = \sigma(y + 2L) = \sigma(-y)$, and $\sigma(y) = k|y|$ for $|y| \leq L$.

The RS space is viewed as bulk AdS space ($0 < y < L$) with AdS curvature $\Lambda = -6k^2$ sandwiched by the Planck (or UV) brane at $y = 0$ and the TeV (or IR) brane at $y = L$. The warp factor $z_L = e^{kL} \gg 1$ is very large ($\sim 10^{15}$). The KK mass scale is given by $m_{\text{KK}} = \pi k / (z_L - 1) \sim \pi k z_L^{-1}$.

In the fundamental region $0 \leq y \leq L$ the metric can be written in terms of the useful conformal coordinate $z = e^{ky}$ as

$$ds^2 = \frac{1}{z^2} \left(\eta_{\mu\nu} dx^\mu dx^\nu + \frac{dz^2}{k^2} \right). \quad (2)$$

The 5D Lagrangian density has following structure:

$$\begin{aligned} \mathcal{L} = & \mathcal{L}_{\text{bulk}}^{\text{gauge}}(A, B) + \mathcal{L}_{\text{bulk}}^{\text{fermion}}(\Psi_a, \Psi_F, A, B) \\ & + \mathcal{L}_{\text{brane}}^{\text{fermion}}(\hat{\chi}_\alpha, A, B) + \mathcal{L}_{\text{brane}}^{\text{scalar}}(\hat{\Phi}, A, B) + \mathcal{L}_{\text{brane}}^{\text{int}}(\Psi_a, \hat{\chi}_\alpha, \hat{\Phi}), \end{aligned} \quad (3)$$

where A_M and B_M are $SO(5)$ and $U(1)_X$ gauge fields with the two associated gauge coupling constants g_A and g_B , respectively; $\Psi_a, a = 1, 2, 3, 4$ are the 5D bulk fermions in the vector representation of $SO(5)$ which contains usual leptons and quarks; Ψ_F are n_F the 5D bulk fermions in the spinor representation of $SO(5)$; $\hat{\chi}_\alpha$ the Planck ($y = 0$) brane fermions in the fundamental representation of $SO(4) \cong SU(2)_L \times SU(2)_R$ (in particular with these brane fermions all 4D anomalies in $SO(4) \times U(1)_X$ are cancelled); $\hat{\Phi}$ are the Planck brane scalars which induces symmetry breaking $SU(2)_R \times U(1)_X$ to $U(1)_Y$ on UV brane $y = 0$.

The explicit view of the all lagrangian density parts can be found in

[7]-[11]. For example, the sum of the bulk matter parts can be written as

$$\begin{aligned}
\mathcal{L}_{\text{bulk}}^{\text{gauge}} + \mathcal{L}_{\text{bulk}}^{\text{fermions}} &= -\text{Tr} \left(\frac{1}{4} F^{(A)MN} F_{MN}^{(A)} + \frac{1}{2\xi_A} (f_{\text{gf}}^{(A)})^2 + \mathcal{L}_{\text{gh}}^{(A)} \right) - \\
&\quad - \left(\frac{1}{4} F^{(B)MN} F_{MN}^{(B)} + \frac{1}{2\xi_B} (f_{\text{gf}}^{(B)})^2 + \mathcal{L}_{\text{gh}}^{(B)} \right) +, \quad (4) \\
&\quad + \sum_a \bar{\Psi}_a \mathcal{D}(c_a) \Psi_a + \sum_{i=1}^{n_F} \bar{\Psi}_{F_i} \mathcal{D}(c_{F_i}) \Psi_{F_i}, \\
\mathcal{D}(c) &= \Gamma^A e_A{}^M \left(\partial_M + \frac{1}{8} \omega_{MBC} [\Gamma^B, \Gamma^C] - \right. \\
&\quad \left. -ig_A A_M - ig_B Q_X B_M \right) - c\epsilon(y), \quad (5)
\end{aligned}$$

where the gauge fixing and ghost terms are denoted as functionals with subscripts gf and gh, respectively. The gauge field strengths are $F_{MN}^{(A)} = \partial_M A_N - \partial_N A_M - ig_A [A_M, A_N]$, $F_{MN}^{(B)} = \partial_M B_N - \partial_N B_M$. The gauge fixing function is taken as $f_{\text{gf}}^{(A)} = z^2 \{ \eta^{\mu\nu} \mathcal{D}_\mu A_\nu + \xi_A k^2 z \mathcal{D}_z^c (A_z^q/z) \}$ with a background field A_z^c ($A_z = A_z^c + A_z^q$), $B_z^c = 0$. In this paper we take $\xi_A = \xi_B = 1$.

The $SO(5)$ gauge fields A_M are decomposed as

$$A_M = \sum_{a_L=1}^3 A_M^{a_L} T^{a_L} + \sum_{a_R=1}^3 A_M^{a_R} T^{a_R} + \sum_{\hat{a}=1}^4 A_M^{\hat{a}} T^{\hat{a}}, \quad (6)$$

where T^{a_L, a_R} ($a_L, a_R = 1, 2, 3$) and $T^{\hat{a}}$ ($\hat{a} = 1, 2, 3, 4$) are the generators of $SO(4) \simeq SU(2)_L \times SU(2)_R$ and $SO(5)/SO(4)$, respectively.

The electric charge satisfies to following equality

$$Q_{\text{EM}} = T^{3L} + T^{3R} + Q_X. \quad (7)$$

In the fermion part we have $\bar{\Psi} = i\Psi^\dagger \Gamma^0$, and Γ^M matrices are given by

$$\Gamma^\mu = \begin{pmatrix} & \sigma^\mu \\ \bar{\sigma}^\mu & \end{pmatrix}, \quad \Gamma^5 = \begin{pmatrix} 1 & \\ & -1 \end{pmatrix}, \quad \sigma^\mu = (1, \vec{\sigma}), \quad \bar{\sigma}^\mu = (-1, \vec{\sigma}). \quad (8)$$

The $c\epsilon(y)$ term in the action, where $\epsilon(y) \equiv \text{sign}(y)$, gives a bulk kink mass. The dimensionless parameter c plays an important role in controlling profiles of fermions wave functions.

The orbifold boundary conditions at $y_0 = 0$ and $y_1 = L$ points are given by following relations

$$\begin{aligned}
\begin{pmatrix} A_\mu \\ A_y \end{pmatrix} (x, y_j - y) &= P_{\text{vec}} \begin{pmatrix} A_\mu \\ -A_y \end{pmatrix} (x, y_j + y) P_{\text{vec}}^{-1}, \\
\begin{pmatrix} B_\mu \\ B_y \end{pmatrix} (x, y_j - y) &= \begin{pmatrix} B_\mu \\ -B_y \end{pmatrix} (x, y_j + y), \\
\Psi_a(x, y_j - y) &= P_{\text{vec}} \Gamma^5 \Psi_a(x, y_j + y), \\
\Psi_{F_i}(x, y_j - y) &= (-1)^j P_{\text{sp}} \Gamma^5 \Psi_{F_i}(x, y_j + y), \\
P_{\text{vec}} &= \text{diag}(-1, -1, -1, -1, +1), \quad P_{\text{sp}} = \text{diag}(+1, +1, -1, -1). \quad (9)
\end{aligned}$$

The Lagrangian density remains invariant under the parity transformations. The $SO(5)$ symmetry is reduced to $SO(4) \simeq SU(2)_L \times SU(2)_R$ by the orbifold boundary conditions. At this stage the four-dimensional components A_μ of the five-dimensional gauge fields A_M have zero modes only in $SO(4) \times U(1)_X$ block, whereas the extra-dimensional components A_y have zero modes only in $SO(5)/SO(4)$ block. The latter contains the four-dimensional Higgs field, which is a doublet concerning both $SU(2)_L$ and $SU(2)_R$ groups:

$$SO(5) : A_y = \begin{pmatrix} \phi_1 \\ \phi_2 \\ \phi_3 \\ \phi_4 \\ -\phi_1 & -\phi_2 & -\phi_3 & -\phi_4 \end{pmatrix}, \quad \Phi = \begin{pmatrix} \phi_1 + i\phi_2 \\ \phi_4 - i\phi_3 \end{pmatrix}. \quad (10)$$

After determination mass spectra of all boson and fermion fields we can find Coleman–Weinberg effective potential. Should be note that 4D Higgs field associated with nontrivial Wilson line phase. The Wilson line phase for the zero modes is defined as

$$e^{i\Theta_H/2} \sim P \exp \left\{ ig_A \int_0^L dy A_y \right\}. \quad (11)$$

At the tree level the value of the Θ_H is not determined, as it gives vanishing field strengths. At the quantum level its effective potential V_{eff} becomes nontrivial. The value of Θ_H is determined by the location of the

minimum of V_{eff} . Without loss of generality one can assume that $(A_y)_{45}$ component develops a non-vanishing expectation value. Let us denote the corresponding component of Θ_H by θ_H . If θ_H takes a non-vanishing value, the electroweak symmetry breaking takes place.

Further for the extra-dimensional component $A_z = (kz)^{-1}A_y$, which contains the four-dimensional Higgs field $H(x)$, we can write down following expansion

$$A_z^{\hat{4}}(x, z) = \{\theta_H f_H + H(x)\} u_H(z) + \dots ,$$

$$u_H(z) = \sqrt{\frac{2}{k(z_L^2 - 1)}} z \quad \text{for } 1 \leq z \leq z_L . \quad (12)$$

The value of θ_H is determined by the location of the global minimum of the effective potential $V_{\text{eff}}(\theta_H)$. The Higgs boson mass is given by

$$m_H^2 = \frac{1}{f_H^2} \left. \frac{d^2 V_{\text{eff}}}{d\theta_H^2} \right|_{\text{min}} , \quad f_H = \frac{2}{g_w} \sqrt{\frac{k}{L(z_L^2 - 1)}} . \quad (13)$$

Let us consider the case in which all $SO(5)$ -spinor fermions Ψ_{F_i} are degenerate at the tree level, so $c_{F_i} = c_F$ ($i = 1, \dots, n_F$). At the one-loop level only the KK towers whose mass spectra depend on θ_H contribute to the effective potential $V_{\text{eff}}(\theta_H)$. These spectra are given for the gauge W and Z tower, for the top and the bottom quark tower, and for D and fermion F tower. Contributions of other quarks and leptons turn out exponentially suppressed and negligible.

The relevant parameters of the model are $k, z_L, g_A, g_B, c_t, \tilde{\mu}/\mu_2, c_F$ and n_F . Other brane mass parameters are irrelevant so long as $\mu_\alpha, \tilde{\mu}, w \gg m_{\text{KK}}$. These eight parameters are chosen such that $m_Z, \alpha_w, \sin^2 \theta_W, m_t, m_b$, and m_H take the observed values. This procedure leaves two parameters z_L and n_F free.

With those given parameters, the one-loop effective potential is given by

$$V_{\text{eff}}(\theta_H, c_t, r_t, c_F, n_F, k, z_L, \theta_W) = 4I[Q_W] + 2I[Q_Z] + 3I[Q_D]$$

$$- 12\{I[Q_{\text{top}}] + I[Q_{\text{bottom}}]\} - 8n_F I[Q_F] ,$$

$$I[Q(q; \theta_H)] = \frac{(kz_L^{-1})^4}{(4\pi)^2} \int_0^\infty dq q^3 \ln\{1 + Q(q; \theta_H)\} ,$$

$$\begin{aligned}
Q_W &= \cos^2 \theta_W Q_Z = \frac{1}{2} Q_D = \frac{1}{2} Q_0[q; \frac{1}{2}] \sin^2 \theta_H , \\
Q_{\text{top}} &= \frac{Q_{\text{bottom}}}{r_t} = \frac{Q_0[q; c_t]}{2(1+r_t)} \sin^2 \theta_H , \\
Q_F &= Q_0[q; c_F] \cos^2 \frac{1}{2} \theta_H , \\
Q_0[q; c] &= \frac{z_L}{q^2 \hat{F}_{c-\frac{1}{2}, c-\frac{1}{2}}(qz_L^{-1}, q) \hat{F}_{c+\frac{1}{2}, c+\frac{1}{2}}(qz_L^{-1}, q)} , \\
\hat{F}_{\alpha, \beta}(u, v) &= I_\alpha(u) K_\beta(v) - e^{-i(\alpha-\beta)\pi} K_\alpha(u) I_\beta(v) , \tag{14}
\end{aligned}$$

where $r_t = (\tilde{\mu}/\mu_2)^2$ and K_α and I_α are modified Bessel functions.

The value $\theta_H = \theta_1$ at the minimum is determined as $\theta_H(z_L, n_F)$. All other quantities such as the mass spectra of all KK towers, gauge couplings of all particles, and Yukawa couplings of all fermions are determined as functions of z_L and n_F .

The example of profile $V_{\text{eff}}(\theta_H)$ is depicted in Fig. 1 with red curves. For comparison V_{eff} in the case of $n_F = 0$ is also plotted with a blue curve. When $n_F = 0$ and $z_L = 10^7$, the minima are located at $\theta_H = \pm \frac{1}{2}\pi$.

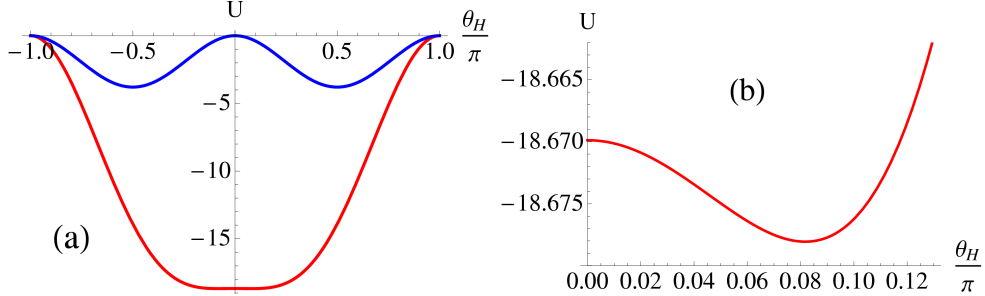


Figure 1: The effective potential $V_{\text{eff}}(\theta_H)$ for $z_L = 10^7$. $U = 16\pi^6 m_{\text{KK}}^{-4} V_{\text{eff}}$ is plotted. The red curves are for $n_F = 3$ with $m_H = 126$ GeV. V_{eff} has minima at $\theta_H = \pm 0.258$ and $m_{\text{KK}} = 3.95$ TeV. The blue curve is for $n_F = 0$ in which case $m_H = 87.9$ GeV and $m_{\text{KK}} = 993$ GeV.

Determined values for θ_H , m_{KK} , $m_{Z^{(1)}}$, etc. are tabulated in Table 2 in the case of $n_F = 5$.

Table 2: Parameters and masses in the case of degenerate dark fermions with $n_F = 5$. All masses and k are given in units of TeV.

z_L	θ_H	m_{KK}	k	c_t	c_F	$m_{F^{(1)}}$	$m_{Z_R^{(1)}}$	$m_{Z^{(1)}}$	$m_{\gamma^{(1)}}$
10^9	0.473	2.50	7.97×10^8	0.376	0.459	0.353	1.92	1.97	1.98
10^8	0.351	3.13	9.97×10^7	0.357	0.445	0.502	2.40	2.48	2.48
10^7	0.251	4.06	1.29×10^7	0.330	0.430	0.735	3.11	3.24	3.24
10^6	0.172	5.45	1.74×10^6	0.292	0.410	1.11	4.17	4.37	4.38
10^5	0.114	7.49	2.38×10^5	0.227	0.382	1.75	5.73	6.07	6.08
10^4	0.0730	10.5	3.33×10^4	0.037	0.333	2.91	8.00	8.61	8.61

3 Phenomenological predictions

One of the distinctive predictions of the $SO(5) \times U(1)$ gauge-Higgs unification is the existence of the KK excited modes of neutral gauge bosons and photon. There are four kinds of neutral gauge bosons at the TeV scale. They are the first KK mode of Z boson $Z^{(1)}$ ($Z^{(0)} \equiv Z^{\text{SM}}$), the first KK mode of photon $\gamma^{(1)}$ ($\gamma^{(0)} \equiv \gamma^{\text{SM}}$), the $Z_R^{(1)}$ boson ($Z_R^{(0)}$ is not exist), the $A^{\hat{4}}$ boson.

Among them the $A^{\hat{4}}$ boson does not couple to SM particles so that it escapes from detection in the Z' search. $Z^{(1)}$, $\gamma^{(1)}$, and $Z_R^{(1)}$ are the candidates for Z' bosons.

To evaluate the production and decay rates of Z' bosons is needed to know four-dimensional Z' couplings of quarks and leptons. They are obtained from the five-dimensional gauge interaction terms by inserting wave functions of gauge bosons and quarks or leptons and integrating over the fifth-dimensional coordinate. The couplings of the photon, Z boson

and $Z_R^{(1)}$ boson KK towers can be written as

$$\begin{aligned}
\mathcal{L} \supset \sum_{n,i} A_\mu^{\gamma^{(n)}} & \left[g_{u^i L}^{\gamma^{(n)}} \bar{u}_L^i \gamma^\mu u_L^i + g_{u^i R}^{\gamma^{(n)}} \bar{u}_R^i \gamma^\mu u_R^i + g_{d^i L}^{\gamma^{(n)}} \bar{d}_L^i \gamma^\mu d_L^i + g_{d^i R}^{\gamma^{(n)}} \bar{d}_R^i \gamma^\mu d_R^i \right. \\
& \left. + g_{e^i L}^{\gamma^{(n)}} \bar{e}_L^i \gamma^\mu e_L^i + g_{e^i R}^{\gamma^{(n)}} \bar{e}_R^i \gamma^\mu e_R^i \right] \\
+ \sum_{n,i} Z_\mu^{(n)} & \left[g_{u^i L}^{Z^{(n)}} \bar{u}_L^i \gamma^\mu u_L^i + g_{u^i R}^{Z^{(n)}} \bar{u}_R^i \gamma^\mu u_R^i + g_{d^i L}^{Z^{(n)}} \bar{d}_L^i \gamma^\mu d_L^i + g_{d^i R}^{Z^{(n)}} \bar{d}_R^i \gamma^\mu d_R^i \right. \\
& \left. + g_{\nu^i L}^{Z^{(n)}} \bar{\nu}_L^i \gamma^\mu \nu_L^i + g_{\nu^i R}^{Z^{(n)}} \bar{\nu}_R^i \gamma^\mu \nu_R^i + g_{e^i L}^{Z^{(n)}} \bar{e}_L^i \gamma^\mu e_L^i + g_{e^i R}^{Z^{(n)}} \bar{e}_R^i \gamma^\mu e_R^i \right] \\
+ \sum_{n,i} Z_{R\mu}^{(n)} & \left[g_{u^i L}^{Z_R^{(n)}} \bar{u}_L^i \gamma^\mu u_L^i + g_{u^i R}^{Z_R^{(n)}} \bar{u}_R^i \gamma^\mu u_R^i + g_{d^i L}^{Z_R^{(n)}} \bar{d}_L^i \gamma^\mu d_L^i + g_{d^i R}^{Z_R^{(n)}} \bar{d}_R^i \gamma^\mu d_R^i \right. \\
& \left. + g_{\nu^i L}^{Z_R^{(n)}} \bar{\nu}_L^i \gamma^\mu \nu_L^i + g_{\nu^i R}^{Z_R^{(n)}} \bar{\nu}_R^i \gamma^\mu \nu_R^i + g_{e^i L}^{Z_R^{(n)}} \bar{e}_L^i \gamma^\mu e_L^i + g_{e^i R}^{Z_R^{(n)}} \bar{e}_R^i \gamma^\mu e_R^i \right],
\end{aligned}$$

where the superscript i denotes the generation, i.e., $(u^1, u^2, u^3) = (u, c, t)$, etc. The four-dimensional gauge couplings are obtained by overlapping integrals of wave functions (which contains the combination of Bessel functions) and cannot be written in simple analytical form. Explicit formulas for the gauge couplings can be found in papers cited above.

The relevant couplings of the Z' bosons for fixing θ_H parameter are tabulated in Table 3 and Table 4.

Table 3: Masses, total decay widths and couplings of the Z' bosons to SM particles in the first generation for $\theta_H = 0.114$. Couplings to μ are approximately the same as those to e .

Z'	$m(\text{TeV})$	$\Gamma(\text{GeV})$	$g_{uL}^{Z'}$	$g_{dL}^{Z'}$	$g_{eL}^{Z'}$	$g_{uR}^{Z'}$	$g_{dR}^{Z'}$	$g_{eR}^{Z'}$
Z	0.0912	2.44	0.257	-0.314	-0.200	-0.115	0.0573	0.172
$Z_R^{(1)}$	5.73	482	0	0	0	0.641	-0.321	-0.978
$Z^{(1)}$	6.07	342	-0.0887	0.108	0.0690	-0.466	0.233	0.711
$\gamma^{(1)}$	6.08	886	-0.0724	0.0362	0.109	0.846	-0.423	-1.29
$Z^{(2)}$	9.14	1.29	-0.0073	0.0089	0.0056	0.0055	0.00274	0.0086

Table 4: Masses, total decay widths and couplings of the Z' bosons to SM particles in the first generation for $\theta_H = 0.073$.

Z'	$m(\text{TeV})$	$\Gamma(\text{GeV})$	$g_{uL}^{Z'}$	$g_{dL}^{Z'}$	$g_{eL}^{Z'}$	$g_{uR}^{Z'}$	$g_{dR}^{Z'}$	$g_{eR}^{Z'}$
$Z_R^{(1)}$	8.00	553	0	0	0	0.588	-0.294	-0.896
$Z^{(1)}$	8.61	494	-0.100	0.123	0.078	-0.426	0.213	0.650
$\gamma^{(1)}$	8.61	1040	-0.0817	0.041	0.123	0.775	-0.388	-1.18

The decay width of the Z' boson is given by

$$\Gamma_{Z'} = \sum_i \frac{m_{Z'}}{12\pi} \left(\frac{(g_{iL}^{Z'})^2 + (g_{iR}^{Z'})^2}{2} + 2g_{iL}^{Z'}g_{iR}^{Z'} \frac{m_i^2}{m_{Z'}^2} \right) \sqrt{1 - \frac{4m_i^2}{m_{Z'}^2}}. \quad (15)$$

Here i runs over all fermions including SM fermions and exotic fermions. The contribution of its decay to W^+W^- is very small and can be neglected. The evaluated $\Gamma_{Z'}$ for $\theta_H = 0.114$ is summarized in Table 3. It is seen that all of $Z_R^{(1)}$, $Z^{(1)}$, and $\gamma^{(1)}$ have large decay widths (300 ~ 900 GeV) in quite contrast to the narrow width of the Z boson. It is mainly due to the large couplings of right-handed quarks and leptons.

Now consider the dilepton production cross sections through the Z' boson exchange together with the SM processes mediated by the Z boson and photon. The dependence of the cross section on the final state dilepton invariant mass $M_{\ell\ell}$ is described as

$$\begin{aligned} \frac{d\sigma(pp \rightarrow \ell^+\ell^- X)}{dM_{\ell\ell}} &= \sum_q \int_{-1}^1 d\cos\theta \int_{\frac{M_{\ell\ell}^2}{E_{\text{CMS}}^2}}^1 dx_1 \frac{2M_{\ell\ell}}{x_1 E_{\text{CMS}}^2} \\ &\times f_q(x_1, M_{\ell\ell}^2) f_{\bar{q}} \left(\frac{M_{\ell\ell}^2}{x_1 E_{\text{CMS}}^2}, M_{\ell\ell}^2 \right) \frac{d\sigma(\bar{q}q \rightarrow \ell^+\ell^-)}{d\cos\theta} \end{aligned} \quad (16)$$

where E_{CMS} is the center-of-mass energy of the LHC and f_q 's are the parton distribution functions(PDFs) for q quark.

Figure 2 shows the differential cross section for $pp \rightarrow \mu^+\mu^-$ together with the SM cross section mediated by the Z boson and photon for $\theta_H = 0.114$ ($n_F = 5$, $z_L = 10^5$). The deviation from the SM is very small below 3 TeV because the couplings of the Z boson or photon to SM fermions

are almost the same as in the SM. For this reason it is difficult to see the signals of the gauge-Higgs unification at 8 TeV LHC experiments. In the case of $\theta_H = 0.251$ ($n_F = 5$, $z_L = 10^7$), the deviation from the SM is large and this value is excluded by the 8 TeV LHC experiments.

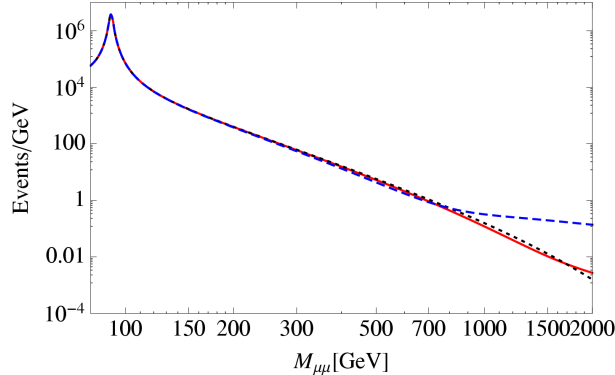


Figure 2: The differential cross section multiplied by an integrated luminosity of 20.6 fb^{-1} for $pp \rightarrow \mu^+ \mu^- X$ at the 8 TeV LHC for $\theta_H = 0.114$ (red solid curve) and for $\theta_H = 0.251$ (blue dashed curve). The black dashed line represents the SM background.

On the other hand, at 14 TeV LHC experiments, we expect the signals. Figure 3 shows the differential cross section $d\sigma/dM_{\mu\mu}$ in the range $3 \text{ TeV} < M_{\mu\mu} < 9 \text{ TeV}$ for $\theta_H = 0.114$ and 0.073 . The contributions from $Z^{(2)}$ boson and higher KK modes are negligible because the couplings are very small and the widths are very narrow (see Table 4). One sees a very large deviation from the SM, which can be detected at the upgraded LHC.

4 Conclusion and remarks

In the $SO(5) \times U(1)$ gauge-Higgs unification the three gauge bosons, $Z_R^{(1)}$, $Z^{(1)}$, and $\gamma^{(1)}$, appear as Z' bosons in dilepton events at LHC. It is interesting that the masses of these bosons turn out around 6 (8 TeV) for $\theta_H = 0.114$ (0.073), which is exactly in the region explored at the 14 TeV LHC.

As right-handed quarks and leptons have large couplings to those Z' bosons, the widths of those bosons become large; the decay widths of $Z_R^{(1)}$,

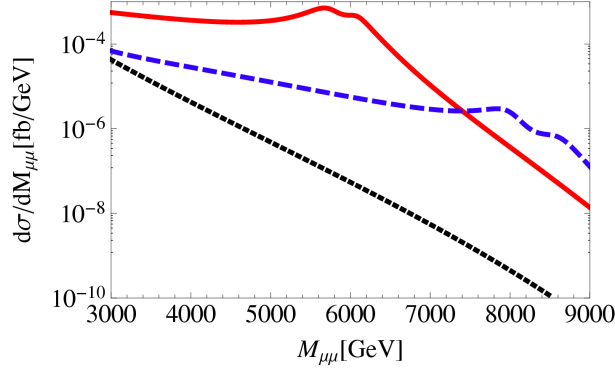


Figure 3: The differential cross section for $pp \rightarrow \mu^+ \mu^- X$ at the 14 TeV LHC for $\theta_H = 0.114$ (red solid curve) and for $\theta_H = 0.073$ (blue dashed curve) . The nearly straight line represents the SM background.

$Z^{(1)}$ and $\gamma^{(1)}$ are 482, 342 and 886 GeV for $\theta_H = 0.114$.

As the difference in masses of $Z^{(1)}$ and $\gamma^{(1)}$ is small, there should appear two peaks in dilepton events. Due to the large widths the excess of events over those expected in the SM should be seen in much wider range of energies. For $\theta_H = 0.114$ an excess due to the broad widths of the Z' resonances should be observed above 3 TeV in the dilepton invariant mass. The discovery of the Z' bosons in the 3-9 TeV range would give strong support for the gauge-Higgs unification, signaling the existence of extra dimensions.

Let's give some remarks concerning Higgs interactions. In realistic GHU models all Higgs couplings HWW , HZZ , $Hc\bar{c}$, $Hb\bar{b}$, $H\tau\bar{\tau}$ are suppressed by a factor $\cos\theta_H$ at the tree level, moreover coupling $HZ\gamma$ is absent on 1-loop level. The corrections to $\Gamma[H \rightarrow \gamma\gamma]$ and $\Gamma[H \rightarrow gg]$ due to KK states amount only to 0.2% for $\theta_H = 0.114$. Hence may conclude that $Br(H \rightarrow j) \sim Br^{\text{SM}}(H \rightarrow j)$, where $j = WW, ZZ, \gamma\gamma, gg, b\bar{b}, c\bar{c}, \tau\bar{\tau}$ and $\sigma^{\text{prod}}(H) \cdot Br(H \rightarrow \gamma\gamma) \sim (\text{SM}) \times \cos^2\theta_H$. The signal strength in the $\gamma\gamma$ production relative to the SM is about $\cos^2\theta_H$. It is about 0.99 for $\theta_H \sim 0.1$. This contrasts to the prediction in the UED models in which the contributions of KK states can add up in the same sign.

References

- [1] G. Aad *et al.* [ATLAS Collaboration], Phys. Lett. B **716**, 1 (2012) [arXiv:1207.7214 [hep-ex]].
- [2] S. Chatrchyan *et al.* [CMS Collaboration], Phys. Lett. B **716**, 30 (2012) [arXiv:1207.7235 [hep-ex]].
- [3] D. B. Fairlie, Phys. Lett. B **82**, 97 (1979).
- [4] D. B. Fairlie, J. Phys. G **5**, L55 (1979).
- [5] P. Forgacs and N. S. Manton, Commun. Math. Phys. **72**, 15 (1980).
- [6] N. S. Manton, Nucl. Phys. B **158**, 141 (1979).
- [7] A. D. Medina, N. R. Shah and C. E. M. Wagner, Phys. Rev. D **76**, 095010 (2007) [arXiv:0706.1281 [hep-ph]].
- [8] M. Carena, A. D. Medina, B. Panes, N. R. Shah and C. E. M. Wagner, Phys. Rev. D **77** (2008) 076003 [arXiv:0712.0095 [hep-ph]].
- [9] Y. Hosotani, K. Oda, T. Ohnuma and Y. Sakamura, Phys. Rev. D **78**, 096002 (2008) [Erratum-ibid. D **79**, 079902 (2009)] [arXiv:0806.0480 [hep-ph]].
- [10] Y. Hosotani, S. Noda and N. Uekusa, Prog. Theor. Phys. **123** (2010) 757 [arXiv:0912.1173 [hep-ph]].
- [11] S. Funatsu, H. Hatanaka, Y. Hosotani, Y. Orikasa and T. Shimotani, Phys. Lett. B **722** (2013) 94 [arXiv:1301.1744 [hep-ph]].